THE JOURNAL OF PHYSICAL CHEMISTRY C

ARTICLE

pubs.acs.org/JPCC

Invisible Cavity of a Polymeric Nanofiber Laser

Sheng Li,*[,†,‡] Wei-Feng Jiang,[†] Yuan-Ping Xu,[†] and Thomas F. George*[,‡]

[†]Department of Physics, Zhejiang Normal University, Jinhua, Zhejiang 321004, China

[‡]Office of the Chancellor and Center for Nanoscience, Departments of Chemistry & Biochemistry and Physics & Astronomy, University of Missouri−St. Louis, St. Louis, Missouri 63121, United States

ABSTRACT: Laser emission based on polymer fibers generally undergoes two unconventional processes, microscopic lattice/electron evolution and localization of light emission. After an external laser pulse/beam is used to pump a conjugated polymer fiber comprised of random polymer chains, such as polythiophene, the external excitation immediately destroys the periodic structure of the polymer chain, with self-inducing of the localized lattice distortion along the polymer chain. Along with the continuous optical pumping, the electron populations of the exciton in a single polymer chain are reversed. The external gain, combined with multiple light-scattering in the fiber, counteracts the leakage due to noncoherent light emission, finally localizing the light in the middle of the bunch. Concurrent with the localization of the polymeric fiber laser, the multiple scattering, instead of phase tuning in the traditional resonator, causes the laser cavity to be comprised of only all randomly distributed polymer chains, and thus to be "invisible".

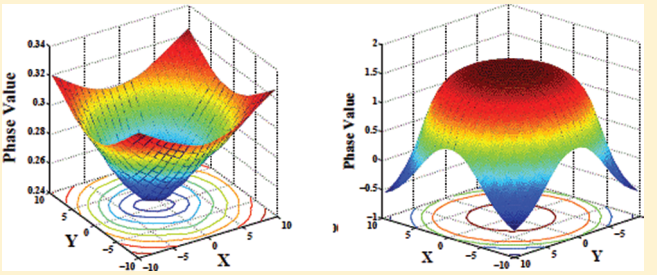

I. INTRODUCTION

The research of polymer lasers dates back to the 1960s when Soffer et al. fabricated a laser based on dye-doped polymers.[1] Accordingly, based on a single crystal of fluorine-doped anthracene, Avanesjan et al. demonstrated the lasing effect.[2] Despite considerable efforts during the 1960s and 1970s,[1−3] the shortage of high-quality organic single crystals still limited the development of polymer lasers. Fortunately, in the 1990s, the invention of polymer light-emitting diodes (PLEDs) broke this limitation.[4,5] In 1992, the first polymeric semiconductor laser was developed in a solution consisting of a conjugated polymer.[6] In 1996, the research was extended to solid conjugated polymers laser,[7−10] where especially Tessler et al. fabricated an optically pumped polymer microcavity laser.[7] Conjugated polymer lasers with a variety of resonators, such as distributed feedback and photonic bandgap structures,[11,12] have been extensively fabricated by using a range of coating and imprinting techniques. This has continued to be a topic of vigorous research, launching a new field known as "plastic lasers".

A plastic laser can be simply depicted as follows: Under external pumping, an electron in the highest-occupied molecular orbital (HOMO) is excited to the lowest-unoccupied molecular orbital (LUMO), with binding to the hole in the HOMO to form an exciton. With continuous external pumping, the stimulated excitation leads to electron population inversion and, subsequently, laser emission.[13] Different from an inorganic laser, the one-dimensional nature of a conjugated polymer causes the polymeric lattice to sensitively depend on the electronic state, self-trapping, which gives the conjugated polymer special flexibility. Taking advantage of this, Quachi and D. O'Carroll fabricated conjugated polymer nanowire lasers based on polythiophene and polyfluorine (PFO) nanofibers.[14,15] Although both are made of conjugated polymer nanofibers, their cavities are different, where the PFO nanofiber laser is comprised of a Fabry−Perot resonator, while the polythiophene nanofiber laser is only made up of some randomly distributed parallel polythiophene nanofibers. Without the help of the resonator, the laser emission of the polythiophene laser is localized on the nanofiber, forming a luminescent spot. The simple structure of the polythiopene nanofiber laser thereby paves the way to fabricate the nanolaser, although it also raises questions as to where to find the "invisible" resonator of the laser and what is the mechanism of the localization of the laser emission. One could assume the localized lasing emission to be attributed to the coherent light propagation in a one-dimensional nanofiber. Yet, on the basis of this assumption, we are unable to exhibit the "hidden" resonator of the laser.

Localized light emission is generally regarded as a collective phenomenon. The electronic behavior, however, is a typical microscopic dynamical process. As compared to the contribution of an exciton to the luminescence of a PLED, scientists have taken it for granted that organic lasing is a similar excitonic behavior.[13] A laser, as a typical excitation of electrons, is triggered by electron population inversion. However, an exciton (electron−hole pair) has no electron population inversion, which is ill-suited to describe the lasing effect. Furthermore, thanks to the self-trapping effect, the occurrence of the lasing effect is also able to induce the change of the lattice structure of the polymer.

Received: July 1, 2011
Revised: August 1, 2011
Published: August 08, 2011

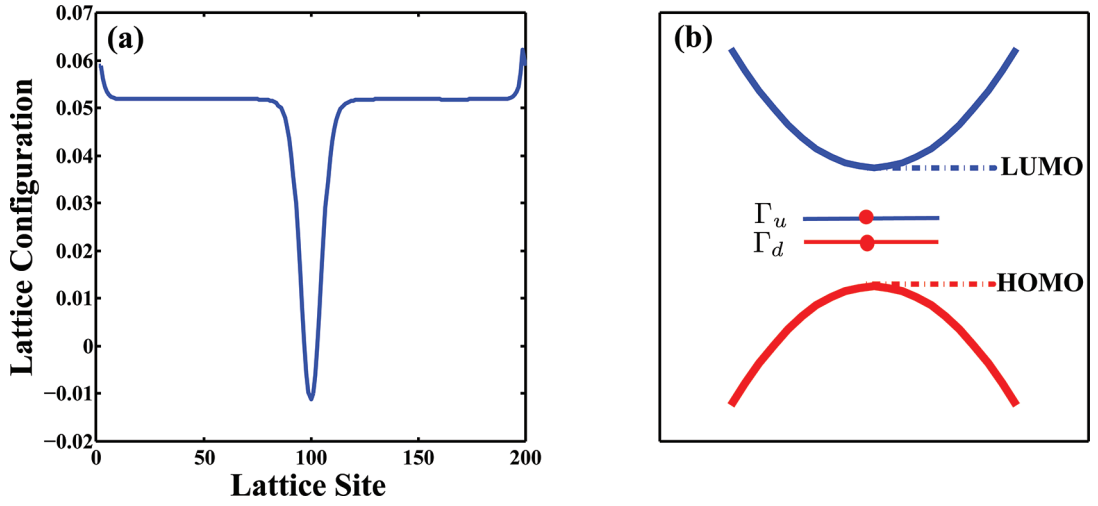

Figure 1. Profile of the singlet exciton: (a) lattice configuration; (b) electronic spectrum. The value of the gap is 5.12 eV, and the energy values of Γ_u and Γ_d are 1.60 and −1.48 eV, respectively.

Therefore, the investigation of the polythiophene nanofiber laser has to involve three strategic effects: self-trapping, electron population inversion, and multiple scattering. How to unite the microscopic behavior with the collective behavior becomes the first key challenge. In this Article, the molecular dynamics and multiple-scattering process are fused together to bridge the gap between the microscopic process and collective behavior, not only describing the electron transition process along with the evolution of lattice structure, but also exhibiting the localized laser emission phenomenon. Further, with a newly developed phase distribution diagram, the invisible resonant cavity is clearly identified.

II. METHOD

We concentrate on the prominent self-trapping of these conjugated polymers, where the extended Hubbard−Su−Schreiffer−Heeger Hamiltonian provides a convenient and accurate description.[16] Because the polymer is not a strongly correlated system, the electron−electron interaction can be treated by the Hartree−Fock approximation.[16] To explore the dynamical properties of carriers in a conjugated polymer, the conventional molecular dynamics combines the electron's behavior and the lattice movement. During the relaxation process associated with the lasing effect, the electronic energy level occupation numbers are changed due to transitions. However, a conventional molecular dynamics approach fixes these occupation numbers, which makes it difficult to describe the electronic transitions of the lasing effect. To resolve this dilemma, we introduce electronic population rate equations into the molecular dynamics treatment following the procedure described in ref 17. Let us assume three occupied electronic energy levels of a single polymer fiber labeled by a, b, and c. Once optical pumping, whose gain is designated by g, pumps an electron in c to a, the evolutions of their related electron populations, P_a, P_b, and P_c, are given as

$$\begin{aligned} dP_a/dt &= gP_c - \gamma_{ab}P_a,\ dP_b/dt = \gamma_{ab}P_a - \gamma_{bc}P_b,\ P_c \\ &= n - P_a - P_b \end{aligned} \quad (1)$$

where γ_{ab} (γ_{bc}) is the transition rate between energy levels a and b (b and c), and n is the total electron number.

When an external laser is focused on a wide-gap polythiophene nanofiber consisting of many randomly distributed parallel polythiophene chains, there is light emission from a polythiophene chain, just like when a dipole oscillates and emits an electromagnetic wave under an external field. Thus, if we represent a polythiophene chain by a linear harmonic oscillator, the polythiophene fiber comprised of parallel polythiophene chains becomes an ensemble of linear harmonic oscillators. Accordingly, the mechanism can be imagined as follows: with the external pumping, every line dipole accepts the external gain. Meanwhile, the electric field generated by all others also drives dipoles to oscillate, thus emitting electromagnetic radiation. Upon repetition, this forms so-called multiple scattering. Thus, we shall assume N identical line dipoles, which are aligned along the z-axis and randomly embedded in a two-dimensional uniform medium, to stand for N parallel polythiophene chains. All lengths are scaled by the average distance between polymer chains. The total electric field driving the kth dipole is comprised of the electric field radiating from the other dipoles, given as

$$E_k = \sum_{j\neq k}^{N} G_j(\vec{r_k} - \vec{r_j}) \quad (2)$$

where $G_j(\vec{r}_k - \vec{r}_j)$ is the electric field experienced by the kth dipole as emitted by the jth line dipoles. Here, the field at every point of the nanofiber can be taken as $E = \vec{e}\,|\vec{E}|e^{i\phi}$. If the phase ϕ of the field in the random medium remains constant, the whole system will behave as a coherent state, exhibiting the property of the lasing effect. Especially, based on the spatial distribution of coherence, the size and shape of the cavity can be clearly illustrated.

Combining the dipole oscillation, threshold behavior of the laser,[18] fusing rate equations, and conventional molecular dynamics, we can quantitatively describe the dynamical evolution of not only the microscopic dynamical process of the polymeric nanofiber, but also the collective behavior of multiple light-scattering in the conjugated polymer chains.

III. RESULTS AND DISCUSSION

For the ground state of the conjugated polymer chain, such as polythiophene, the symmetry-breaking caused by self-trapping

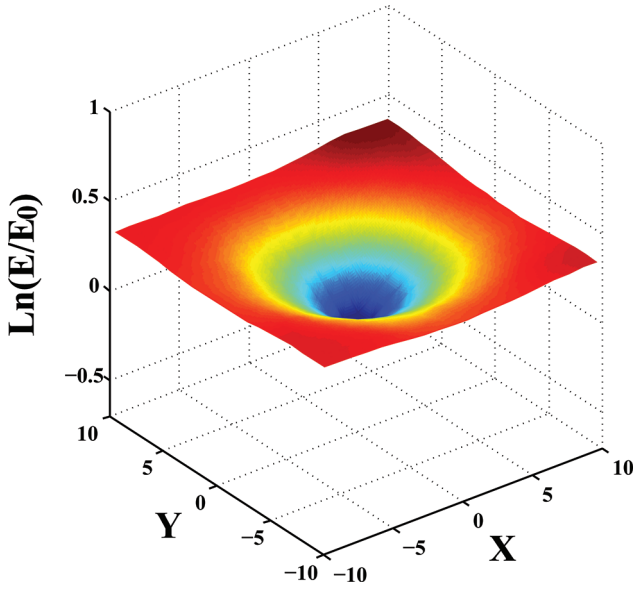

Figure 2. Electric field intensity spatial distribution of light emitted by the nanofiber during the formation of the singlet exciton, where E_0 is the electric field intensity in the center of film. All lengths are scaled by the average distance between polymer chains.

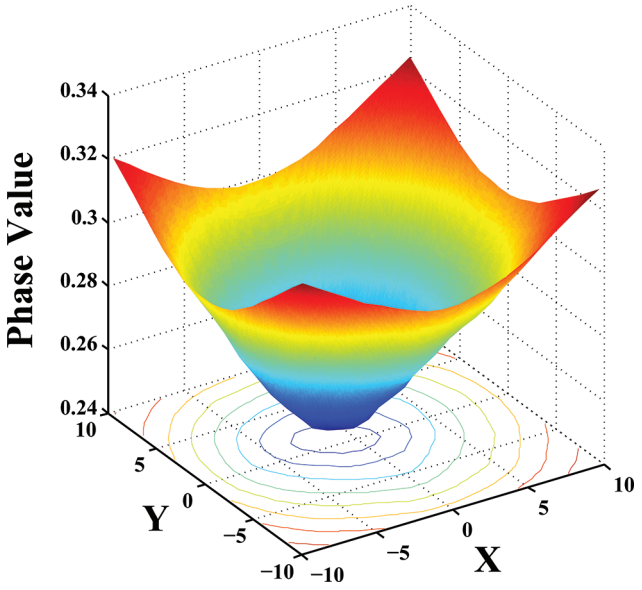

Figure 3. Phase spatial distribution of the light field during the formation of the singlet exciton in the nanofiber. All lengths are scaled by the average distance between polymer chains.

drives the unit clusters/groups to move with different directions. Also, the unit clusters/groups of the conjugated polymer alternate between single and double bonds, thus forming lattice dimerization. The homogeneous dimerization of the lattice structure produces a gap between the HOMO and LUMO. Once an external laser beam or pulse is applied to polythiophene, an electron is easily excited from the HOMO to the LUMO. Near 50 fs, it is found that the original periodic lattice is rapidly destroyed. After 300 fs, a localized lattice distortion appears over the background of the homogeneous dimerization, leading

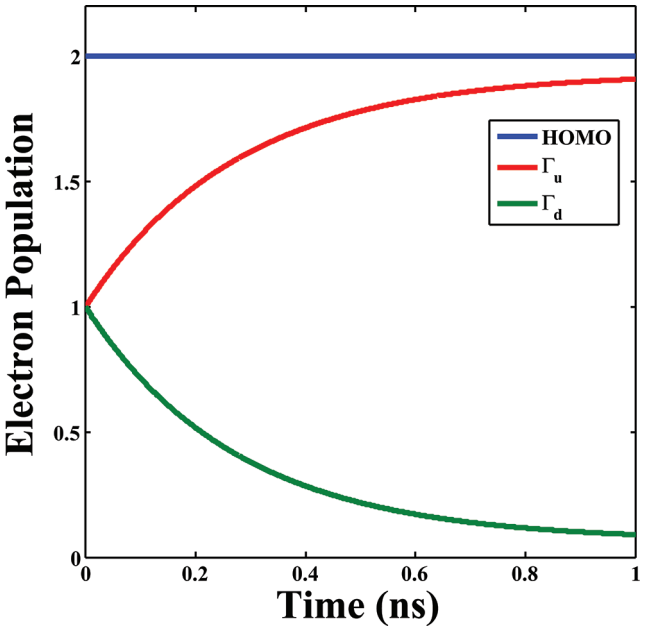

Figure 4. Time-dependent electron populations of three energy levels, HOMO, Γ_u, and Γ_d, of a conjugated polymer semiconductor after it undergoes external optical pumping until population inversion between Γ_u and Γ_d.

ultimately to a stable lattice distortion along with the polymer chain. Associated with the localized lattice distortion, the prominent self-trapping effect of the polymer moves the HOMO and LUMO states to the center of gap, as illustrated in Figure 1a, giving two localized energy levels Γ_u and Γ_d at the center of gap, as shown in Figure 1b. Thus, both lattice distortion and two localized states jointly contribute to form a singlet exciton.

During the formation of the singlet exciton, the light emitted by each polythiophene chain also propagates inside the nanofiber, leading to multiple scattering between polymer chains. Here, the focus is on its energy spatial distribution. As seen in Figure 2, the electric field intensity of light emission is spatially extensive. We randomly choose the detector positions in the fiber to describe the phase distribution of the light field with which the phase ϕ is associated. Interestingly, as shown in Figure 3, the phase of the emitting light is not prone to a certain value, which means that when the singlet exciton contributes to light emission, the polythiophene nanofiber radiates noncoherent light, which, apparently, does not reflect the behavior of the lasing effect. According to the electronic structure of the exciton in Figure 1b, it is predictable that lasing does not exist because there is no electron population inversion, where each of the localized states is occupied by one electron. The singlet exciton only contributes to light emission, not to the lasing effect, which is consistent with the phase spatial distribution of the light emission.

As shown in Figure 1b, two localized energy levels of the singlet exciton and the HOMO provide the appropriate energy structure for lasing in semiconductors. At the beginning, an electron−hole pair forms the exciton. With the continuous pumping of an external optical pulse/beam whose energy matches the difference between Γ_u and the HOMO and exceeds a threshold value, the original microscopic structure of the singlet exciton excitation begins to be changed. First, when the time

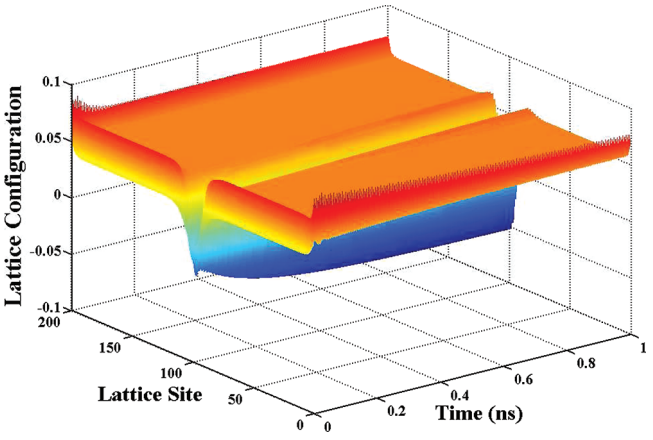

Figure 5. Three-dimensional depiction of the time-dependent lattice configuration induced by external optical pumping over the entire time range.

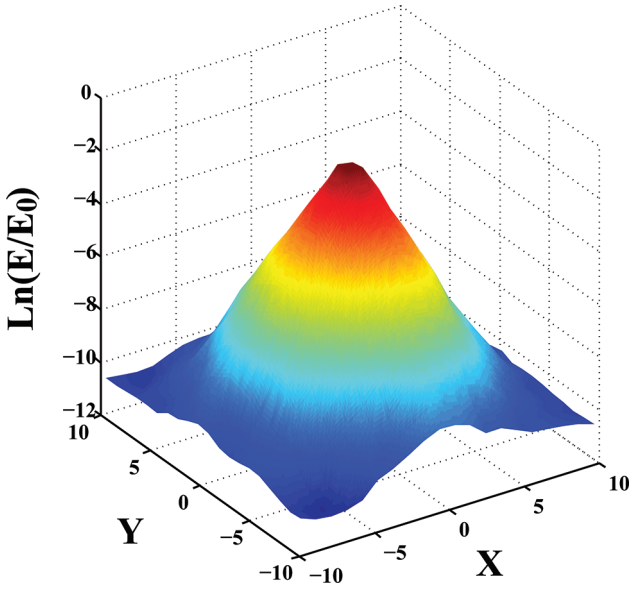

Figure 6. Localized electric field intensity spatial distribution of the light field inside the randomly distributed polymer chains after electron population inversion occurs, where E_0 is the electric field intensity at the center of the nanofiber. All lengths are scaled by the average distance between polymer chains.

reaches 100 ps, the electron population of the HOMO still remains 2, yet the electron population of Γ_u changes to 1.48, while that of Γ_d becomes 0.52, as depicted in Figure 4. During the evolution of the electron population, according to Figure 5, the associated lattice distortion of the conjugated polymer chain becomes more severe than that of the singlet exciton, especially in the first 300 fs. Up to 300 ps, the electron population of Γ_u with higher energy becomes larger than that of Γ_d. The electron population undergoes inversion, manifesting the occurrence of lasing in the single nanothiophene fiber. At 500 ps, the end of the excitation of the singlet exciton, the electron populations become stable, with values of 1.91 and 0.09 for Γ_u and Γ_d, respectively, while the electron population of the HOMO still remains at 2. The stable electron population inversion of the two localized

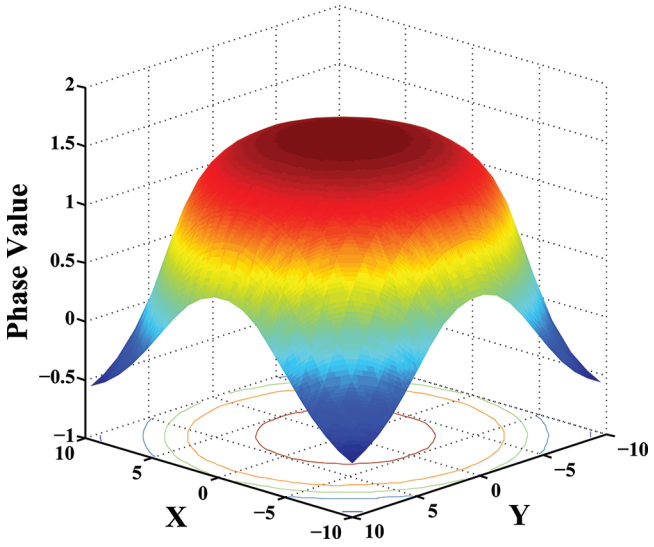

Figure 7. Phase spatial distribution of the light field after electron population inversion occurs in the nanofiber. All lengths are scaled by the average distance between polymer chains.

states, as the microscopic signature of lasing, sustains laser emission of the single polymeric chain.

After surpassing the threshold, the external gain not only induces electron population inversion, but also counteracts the leakage caused by the noncoherent extensive modes. Naturally, when the laser light emitted by each nanothiophene chain propagates inside the fiber, the collective behavior of light emitting in the nanothiophene fiber also should be changed. Thus, the strong multiple scattering has to self-select a new mode without energy leakage to emission. As characterized in Figure 6, the original extensive spatial distribution of the light field disappears, and the light is well-confined insider the fiber, which is consistent with the experimental observation.[14]

Turning to the phase distribution of the light emission, we show the coherence behavior of the light emitted by the fiber in Figure 7: Most of the phase of the entire light field is inclined to a specific value of 1.5, indicating the whole system to have a novel collective behavior. In other words, once the gain exceeds a critical value, besides light localization, the multiple scattering forces most of the thiophene chain to emit light with the same phase of 1.5. Accordingly, the "invisible" cavity for the lasing is comprised of randomly distributed parallel nanothiophene chains. The red zone with the same phase, illustrated in Figure 6, depicts the size of the resonator.

IV. CONCLUSION

In summary, the molecular dynamics and multiple-scattering process are fused together in this Article, which not only describes the electron transition process along with the evolution of lattice structure, but also exhibits the localized laser emission phenomenon. It is found that after a conjugated polymer fiber comprised of random parallel polymer chains, such as polythiophene fibers, is subjected to optical excitation, a singlet exciton is initially formed. The light propagation inside the nanofiber leads to conventional light emission. Yet, with continuous optical pumping, the electron populations of the singlet exciton undergo inversion as well as generate localized lattice distortion. Through multiple light scattering, the nanofiber selects a coherent

dx.doi.org/10.1021/jp206234h |J. Phys. Chem. C 2011, 115, 17582–17586

and localized mode to emit laser radiation, where the resonator consists of randomly distributed parallel polythiophene chains.

AUTHOR INFORMATION

Corresponding Author
*E-mail: shenglee@zjnu.cn (S.L.); tfgeorge@umsl.edu (T.F.G.).

ACKNOWLEDGMENT

We thank S. Y. Liu and X. Sun for helpful discussions. This work was supported by the National Science Foundation of China under Grants 20804039 and 21074118, and the Zhejiang Provincial Qianjiang Talent Project of China under Grant 2010R10019.

REFERENCES

(1) Soffer, B. H.; McFarland, B. B. *Appl. Phys. Lett.* **1967**, *10*, 266–267.
(2) Avanesjan, O. S.; Benderskii, V. A.; Brikenstein, V. K.; Broude, V. L.; Korshunov, L. I.; Lavrushko, A. G.; Tartakovskii, I. I. *Mol. Cryst. Liq. Cryst.* **1974**, *29*, 165–174.
(3) Karl, N. *Phys. Status Solidi A* **1972**, *13*, 651655.
(4) Burroughes, J. H.; Bradley, D. D. C.; Brown, A. R.; Marks, R. N.; Mackay, K.; Friend, R. H.; Burns, P. L.; Holmes, A. B. *Nature* **1990**, *347*, 539–541.
(5) Friend, R. H.; Gymer, R. W.; Holmes, A. B.; Burroughes, J. H.; Marks, R. N.; Taliani, C.; Bradley, D. D. C.; Dos Santos, D. A.; Bredas, J. L.; Logdlund, M.; Salaneck, W. R. *Nature* **1999**, *397*, 121–128.
(6) Moses, D. *Appl. Phys. Lett.* **1992**, *60*, 3215–3216.
(7) Tessler, N.; Denton, G. J.; Friend, R. H. *Nature* **1996**, *382*, 695–697.
(8) Hide, F.; DiazGarcia, M. A.; Schwartz, B. J.; Andersson, M. R.; Pei, Q. B.; Heeger, A. J. *Science* **1996**, *273*, 1833–1836.
(9) Holzer, W.; Penzkofer, A.; Gong, S. H.; Bleyer, A.; Bradley, D. D. C. *Adv. Mater.* **1996**, *8*, 974–978.
(10) Frolov, S. V.; Ozaki, M.; Gellermann, W.; Vardeny, Z. V.; Yoshino, K. *Jpn. J. Appl. Phys., Part 2* **1996**, *35*, L1371–1373.
(11) Heliotis, G.; Xia, R. D.; Turnbull, G. A.; Andrew, P.; Barnes, W. L.; Samuel, I. D. W.; Bradley, D. D. C. *Adv. Funct. Mater.* **2004**, *14*, 91–97.
(12) Riechel, S.; Kallinger, C.; Lemmer, U.; Feldmann, J.; Gombert, A.; Wittwer, V.; Scherf, U. *Appl. Phys. Lett.* **2000**, *77*, 2310–2312.
(13) Samuel, I. D. W.; Turnbull, G. A. *Chem. Rev.* **2007**, *107*, 1272–1295.
(14) Quochi, F.; Cordella, F.; Mura, A.; Bongiovanni, G.; Balzer, F.; Rubahn, H. G. *J. Phys. Chem. B* **2005**, *109*, 21690–12693.
(15) O'Carroll, D.; Lieberwirth, I.; Redmond, G. *Nat. Nanotechnol.* **2007**, *2*, 180–184.
(16) Li, S.; He, X. L.; George, T. F.; Xie, B. P.; Sun, X. *J. Phys. Chem. B* **2009**, *113*, 400–404.
(17) Li, S.; George, T. F. *J. Phys. Chem. B* **2010**, *114*, 8894–8899.
(18) Burin, A. L.; Ratner, M. A.; Cao, H.; Chang, R. P. H. *Phys. Rev. Lett.* **2001**, *87*, 215503-1–4. **2002**, *88*, 093904-1–4.